

000 001 002 003 004 005 ALIGNSEP: TEMPORALLY-ALIGNED VIDEO-QUERIED 006 SOUND SEPARATION WITH FLOW MATCHING 007 008 009

010 **Anonymous authors**
011 Paper under double-blind review
012
013
014
015
016
017
018
019
020
021
022
023
024
025
026
027
028
029

ABSTRACT

030 Video Query Sound Separation (VQSS) aims to isolate target sounds conditioned
031 on visual queries while suppressing off-screen interference—a task central to audiovisual
032 understanding. However, existing methods often fail under conditions of homogeneous
033 interference and overlapping soundtracks, due to limited temporal modeling and weak audiovisual alignment. We propose **AlignSep**, the first
034 generative VQSS model based on flow matching, designed to address common
035 issues such as spectral holes and incomplete separation. To better capture cross-
036 modal correspondence, we introduce a series of temporal consistency mechanisms
037 that guide the vector field estimator toward learning robust audiovisual alignment,
038 enabling accurate and resilient separation in complex scenes. As a *multi-conditioned generation* task,
039 VQSS presents unique challenges that differ fundamentally from traditional flow matching setups. We provide an in-depth analysis
040 of these differences and their implications for generative modeling. To systematically evaluate performance under realistic and difficult conditions, we further
041 construct **VGGSound-Hard**, a challenging benchmark composed entirely of separation
042 cases with homogeneous interference and strong reliance on temporal visual cues. Extensive experiments across multiple benchmarks demonstrate that
043 AlignSep achieves state-of-the-art performance both quantitatively and perceptually,
044 validating its practical value for real-world applications. More results and
045 audio examples are available at: <https://AlignSep.github.io>.
046

1 INTRODUCTION

047 Video-Queried Sound Separation (VQSS) (Tzinis et al., 2022; Chen et al., 2023; Dong et al., 2022;
048 Cheng et al., 2024) aims to isolate sound sources that correspond to visual content in a video while
049 suppressing off-screen interference. As a core task in audio-visual understanding, VQSS facilitates
050 applications such as video editing, accessibility enhancement, and content analysis. Early work in
051 sound separation (Wang & Chen, 2018; Pegg et al., 2023) focused primarily on speech, addressing
052 the classic *cocktail party problem*—separating clean speech from noisy environments. While
053 traditional unsupervised methods (Roweis, 2000; Kristjansson et al., 2006; Hershey et al., 2016) advanced
054 speech separation, they often struggled with interference from sources with similar timbres.
055 To overcome this, researchers introduced visual speech enhancement (Gao & Grauman, 2021; Hsu
056 et al., 2023; Lei et al., 2024), enabling more accurate separation in visually grounded contexts.
057

058 As the field evolved, research expanded beyond speech to more diverse sound sources in complex
059 real-world environments (Kavalerov et al., 2019; Liu et al., 2023b), including instrument separation
060 (Défossez et al., 2019; Luo & Yu, 2023) and general-purpose audio disentanglement (Wisdom
061 et al., 2020). To increase flexibility, multimodal query approaches emerged (Liu et al., 2024; Ma
062 et al., 2024), using text to describe target sounds. However, text descriptions often fail to fully
063 capture the nuances of real-world sound-producing objects and events. This limitation has led to a
064 resurgence of interest in video-guided sound separation, where visual information provides a richer
065 and more precise grounding for identifying target audio sources.
066

067 Despite these advances, current video-guided sound separation methods still face two key limita-
068 tions (Figure 1): **(1) Lack of Temporal Modeling.** Most existing models (Dong et al., 2022; Cheng
069 et al., 2024) rely heavily on semantic cues, which are insufficient for separating acoustically similar
070 sources. For instance, distinguishing multiple barking dogs across on-screen and off-screen regions
071

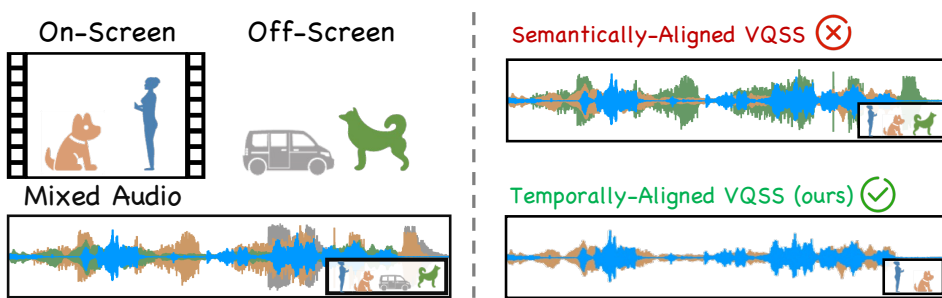


Figure 1: **Comparison of different video-queried sound separation methods.** Traditional category-based methods rely solely on semantic information, struggling to distinguish same-source sounds across on/off-screen regions (e.g., multiple dogs barking). In contrast, our proposed AlignSep can capture audiovisual consistency, enabling precise separation of on/off-screen sounds.

requires capturing temporal alignment between visual motions and corresponding audio energy, not just semantic categories. **(2) Limitations of Mask-Based Methods.** The dominant separation paradigm uses time–frequency masking (Liu et al., 2023b; Chen et al., 2023), which struggles with overlapping soundtracks. In scenarios where multiple sources overlap in both time and frequency, mask-based methods fail to recover clean and distinct signals (Yuan et al., 2024), leading to incomplete separation or artifacts.

To address the aforementioned challenges, we propose **AlignSep**—the first generative temporal-aligned video-queried sound separation model based on flow matching (Lipman et al., 2022) designed for robust audiovisual separation. Unlike prior generative separation models (Yuan et al., 2024; Wang et al., 2024a), VQSS requires maintaining precise temporal alignment between audio and visual streams. To this end, we design a dedicated vector field estimator that explicitly preserves audio-visual alignment by employing a simple yet effective temporal concatenation strategy, combined with a **cross-attention-free feed-forward** Transformer encoder to enforce temporal consistency across modalities. Furthermore, unlike traditional flow-matching tasks—which are typically single-conditioned (e.g., text-to-audio (Huang et al., 2023; Liu et al., 2023a), text-to-image (Zhang et al., 2023) and video-to-audio (Wang et al., 2024b))—VQSS is a multi-conditioned generation task, where both the raw noisy audio and the video sequence jointly condition the output. This fundamental difference leads to new challenges in vector field learning and transport path modeling. We provide an in-depth analysis of these differences, and explain why straightforward rectification and deterministic acceleration techniques (e.g., in rectified flow) are suboptimal in this multi-conditioned setting. We further discuss the trade-offs between performance and efficiency specific to sound separation tasks under these constraints. To facilitate rigorous evaluation of VQSS models under realistic and difficult conditions, we construct **VGGSound-Hard**, a novel benchmark composed entirely of separation cases involving homogeneous interference and strong reliance on fine-grained temporal visual cues. Experimental results on multiple benchmarks—including MUSIC-Clean (Dong et al., 2022), VGGSound-Clean (Dong et al., 2022), and the proposed VGGSound-Hard—demonstrate the effectiveness of AlignSep, highlighting its potential as a next-generation framework for video-guided sound separation. Our main contributions are as follows:

- We revisit the task of video-queried sound separation (VQSS) and provide a detailed analysis of its unique challenges, including homogeneous interference, overlapping soundtracks, and the need for precise audio-visual temporal alignment.
- We propose **AlignSep**, a novel generative temporal-aligned VQSS framework based on conditional flow matching, designed to robustly model multi-conditioned generation by leveraging temporal visual cues and preserving cross-modal consistency.
- We introduce **VGGSound-Hard**, a new benchmark specifically curated to evaluate temporal alignment under real-world homogeneous interference, consisting of co-occurring on-/off-screen same-category sound sources.
- Extensive experiments on three benchmarks—MUSIC-Clean, VGGSound-Clean, and VGGSound-Hard—demonstrate that AlignSep achieves state-of-the-art performance in both quantitative metrics and human perceptual scores (e.g., MOS), validating its effectiveness in real-world audiovisual separation tasks.

108 **2 RELATED WORKS**109 **2.1 UNIVERSAL SOUND SEPARATION**

110 Universal sound separation (Kavalerov et al., 2019; Liu et al., 2022; Pons et al., 2024) aims to
 111 extract distinct audio tracks from mixed signals, serving as a fundamental task for audio under-
 112 standing. Early research primarily focused on domain-specific separation, particularly in speech (Li
 113 et al., 2023; Pegg et al., 2023; Wang et al., 2023; Li et al., 2022) and music (Défossez et al., 2019;
 114 Manilow et al., 2022; Rouard et al., 2023; Luo & Yu, 2023) separation. Subsequent work (Kavalerov
 115 et al., 2019) introduced Permutation Invariant Training (Yu et al., 2017) to separate mixed audio into
 116 multiple unidentified categories. However, these methods are largely limited to music, speech, and
 117 artificial sounds, struggling with complex real-world auditory scenes. To address this, researchers
 118 have developed large-scale annotated audio datasets (Gemmeke et al., 2017; Chen et al., 2020),
 119 advancing universal sound separation. Recent approaches (Ochiai et al., 2020; Kong et al., 2020;
 120 Liu et al., 2022) leverage class labels as queries for targeted sound separation. Nevertheless, tex-
 121 tual descriptions inherently lack the capacity to fully characterize real-world auditory information,
 122 prompting exploration of visual-queried sound separation. We revisit the task of video-queried sound
 123 separation (VQSS) and provide a detailed analysis of its unique challenges, including homogeneous
 124 interference, overlapping soundtracks, and the need for precise audio-visual temporal alignment.

125 **2.2 VISUAL-QUERIED SOUND SEPARATION**

126 In the field of visual-queried sound separation, AudioScope 1&2 (Tzinis et al., 2020; 2022) intro-
 127 duce a novel joint audio-visual classifier to identify object categories that appear in the video and
 128 produce the corresponding sounds in the audio track. Building upon this foundation, i-Query (Chen
 129 et al., 2023) employs an advanced cross-attention mechanism to detect sound-emitting objects within
 130 video sequences, though it relies on pre-extracted object bounding boxes as input. Recent advan-
 131 tages (Dong et al., 2022; Cheng et al., 2024) leveraged powerful visual pre-trained models to ex-
 132 tract rich semantic information from visual content. However, current VQSS methods (Tzinis et al.,
 133 2022; Chen et al., 2023; Dong et al., 2022; Cheng et al., 2024) focus heavily on spatial features
 134 but neglect audio-visual temporal alignment, leading to ambiguity in distinguishing sounds from
 135 on-screen versus off-screen objects of the same category. To address this challenge, we introduce
 136 VGGSound-Hard, a new benchmark specifically curated to evaluate temporal alignment under real-
 137 world homogeneous interference, consisting of co-occurring on-/off-screen same-category sound
 138 sources.

139 **2.3 GENERATIVE SOUND SEPARATION**

140 Traditional sound separation methods (Dong et al., 2022; Cheng et al., 2024) often struggle with
 141 overlapping sound events, as mask-based discriminative models may produce spectral holes (Wang
 142 et al., 2022), limiting their effectiveness in complex acoustic environments. To address this, re-
 143 searchers have turned to non-discriminative models, initially leveraging Generative Adversarial Net-
 144 works (GANs) (Chen et al., 2024) to improve perceptual quality. Subsequent work has explored
 145 diffusion models (Hai et al., 2024) and flow-matching (Yuan et al., 2024) for more natural and re-
 146 fined separation. Despite these advancements, generative visual-queried sound separation remains
 147 unexplored. Inspired by vision-to-audio generation (Wang et al., 2025), we propose AlignSep, a
 148 novel generative VQSS framework based on conditional flow matching, designed to robustly model
 149 multi-conditioned generation by leveraging temporal visual cues and preserving cross-modal con-
 150 sistency.

151 **3 ALIGNSEP**152 **3.1 OVERVIEW**

153 Let a mixed audio signal $A^m = \{A_1^m, \dots, A_n^m\}$ be a linear superposition of a clean audio source
 154 $A^c = \{A_1^c, \dots, A_n^c\}$ and an interfering audio source $A^i = \{A_1^i, \dots, A_n^i\}$. Video-Queried Sound
 155 Separation (VQSS) aims to extract a clean audio signal A^c that maintains strict temporal alignment
 156 with the corresponding visual frame sequence $V = \{V_1, \dots, V_k\}$, where n and k denote the number

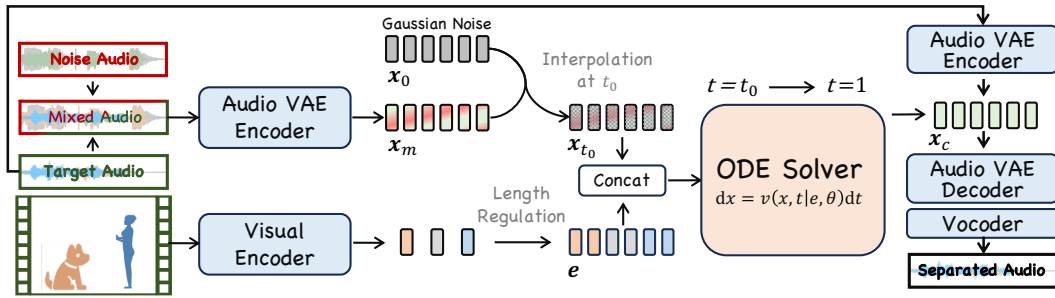


Figure 2: Illustration of AlignSep. AlignSep is a video-queried sound separation model based on flow-matching, designed to establish a mapping from the distribution of mixed audio and the distribution of separated audio, conditioned on visual information. Given a mixed audio input, we first perturb it with Gaussian noise and then progressively denoises it, guided by the visual condition c . This process gradually transforms the mixed noisy audio into separated audio that is temporally aligned with the driving video.

of audio frames and video frames, respectively. As illustrated in Figure 2, we introduce AlignSep, a conditional flow-matching framework designed for precisely temporal-aligned video-queried sound separation. In Section 3.2, we provide a detailed introduction of the flow-matching-based sound separation model. Section 3.3 elaborates on the architectural details of AlignSep, while Sections 3.4 and 3.5 present specialized training strategies aimed at enhancing cross-modal alignment capabilities.

3.2 FLOW-MATCHING BASED SOUND SEPARATION

Conditional sound separation tasks, such as TQSS (Liu et al., 2022) and IQSS (Dong et al., 2022), can be formulated as a conditional mapping from the distribution of mixed audio, $\mathbf{x}_m \sim p_m(\mathbf{x})$, to the distribution of clean audio, $\mathbf{x}_c \sim p_c(\mathbf{x})$. This process can be interpreted as a time-dependent probability density transformation (i.e., flow), governed by the following ordinary differential equation (ODE):

$$d\mathbf{x} = \mathbf{u}(\mathbf{x}, t, e)dt, \quad t \in [0, 1] \quad (1)$$

where t represents the time position, \mathbf{x} is a point in the probability density space at time t , \mathbf{u} denotes the transport vector field (i.e., the probability gradient with respect to t), and e is the conditioning embedding. In Video-Queried Sound Separation (VQSS), the conditioning signal e corresponds to visual features extracted from video frames. The source distribution \mathbf{x}_m and target distribution \mathbf{x}_c represent the compressed mel-spectrogram latents of the mixed audio A^m and clean audio A^c , respectively, obtained via a pre-trained VAE encoder (Liu et al., 2023a).

Conditional Flow Matching Model. The fundamental principle of flow-matching generative model is to train a neural network θ to approximate the transport vector field \mathbf{u} with the flow-matching objective:

$$L_{\text{FM}}(\theta) = \mathbb{E}_{t, p_t(\mathbf{x})} \|v(\mathbf{x}, t, e; \theta) - \mathbf{u}(\mathbf{x}, t, e)\|^2, \quad (2)$$

where $p_t(\mathbf{x})$ denotes the distribution of \mathbf{x} at timestep t . However, in practice, directly computing $\mathbf{u}(\mathbf{x}, t, e)$ is intractable due to the lack of explicit knowledge of the target distribution $p_c(\mathbf{x})$, as well as the unknown forms of $p_t(\mathbf{x})$ and \mathbf{u} . To circumvent this challenge, we adopt the conditional flow-matching (CFM) objective (Lipman et al., 2022), designing specific probabilistic paths that enable efficient sampling from $p_t(\mathbf{x} | \mathbf{x}_c)$ and facilitate the computation of $u(\mathbf{x}, e, t | \mathbf{x}_c)$:

$$L_{\text{CFM}}(\theta) = \mathbb{E}_{t, p_c(\mathbf{x}_c), p_t(\mathbf{x}, \mathbf{x}_c)} \|v(\mathbf{x}, t, e; \theta) - \mathbf{u}(\mathbf{x}, t, \mathbf{x}_c, e)\|^2. \quad (3)$$

ODE Solving and Audio Reconstruction. Once the latent field estimator θ is trained, we use numerical solvers to approximate the solution of the ODE $d\mathbf{x} = v(\mathbf{x}, t, e; \theta)$ at discretized time steps. A simple yet widely used solver is the Euler method, which updates \mathbf{x} iteratively as follows:

$$\mathbf{x}_{t+\epsilon} = \mathbf{x} + \epsilon v(\mathbf{x}, t, e; \theta) \quad (4)$$

where ϵ is the step size. Finally, the sampled latent representation is passed through the VAE decoder to reconstruct the mel-spectrogram, followed by a vocoder (Lee et al., 2022) to generate the final audio waveform.

216 3.3 DETAILED MODEL ARCHITECTURE
217

218 **Audio Encoder & Visual Encoder.** To achieve effective temporal encoding of video sequences, we
219 employ the pre-trained temporal visual encoder (CAVP) from prior V2A work (Luo et al., 2023).
220 Distinguished from the global-level representation like ImageBind (Han et al., 2023) that primarily
221 focus on semantic content representation, CAVP incorporates temporal synchronization supervision
222 between video and audio modalities. This enables the encoder to capture dynamic temporal cor-
223 relations across video frames, rather than relying solely on static semantic features. As for audio
224 modality, to align the distributions of mixed and clean audio as closely as possible, we use a pre-
225 trained VAE audio encoder (Liu et al., 2023a) to map both into a shared audio latent space. During
226 inference, the paired VAE decoder can then directly convert the latent features back into mel spec-
227 trograms.

228 **Temporally-Aligned Vector Field Estimator.** As the core component of our model, the vector
229 field estimator employs a feedforward Transformer architecture. Given the critical importance of
230 temporal alignment, we adopt a concatenation-based approach to effectively fuse multimodal fea-
231 tures. Specifically, after extracting video features e , which has a dimension of 512, via CAVP and
232 latent-space audio features x_m , which has a dimension of 20, via VAE, we first expand the video fea-
233 tures to match the time dimension of the audio features, ensuring precise temporal correspondence.
234 These aligned features are then concatenated, followed by the timestep-encoded vector t appended
235 at the end of the sequence. This structured input is subsequently fed into the main model for noise
236 prediction, allowing it to leverage temporally coherent information for improved performance.

237 3.4 CLASSIFIER-FREE GUIDANCE
238

239 For our generative sound separation task, it can be considered a variant of a video-to-audio task.
240 Therefore, we employ classifier-free guidance. This method effectively combines conditional and
241 unconditional output, allowing us to strike a balance between quality and diversity. The sampling
242 procedure for our audio generation with classifier-free guidance can be formulated as follows:

$$\hat{v}(x, t, e; \theta) = s \cdot v(x, t, e; \theta) + (1 - s) \cdot v(x, t, \emptyset; \theta) \quad (5)$$

243 Here, $s > 1$ represents the classifier sampling scale, which adjusts the balance between the diversity
244 and quality of the generated samples. The ODE solver conditioned with \emptyset is realized by randomly
245 dropping the latent variable e and replacing it with a "null" embedded representation. This latent
246 input exchange facilitates the sampling procedure for video-to-audio generation, as we have estab-
247 lished a modality-aligned latent space. We set s to 4.5 in our experiments.

248 4 VGG SOUND-HARD: A BENCHMARK FOR SOUND SEPARATION UNDER
249 HOMOGENEOUS REAL-WORLD INTERFERENCE250 4.1 HOMOGENEOUS AUDIO PAIR CONSTRUCTION
251

252 All samples in VGGSound-Hard are sourced from the VGGSound test set. To construct mixtures
253 with **homogeneous real-world interference**, we first group audio clips by their category labels.
254 Within each category, we compute pairwise cosine similarity using the CLAP audio encoder and
255 select the highest-scoring pairs, yielding approximately 2,000 candidate homogeneous audio pairs.
256 Following the synthesis pipeline of CLIPSep (Dong et al., 2022), each same-category pair is then
257 mixed to produce a preliminary set of homogeneous mixed-audio samples.

258 4.2 HUMAN VERIFICATION
259

260 To ensure that the final data reliably supports the evaluation of **temporal alignment in sound sep-
261 aration**, we perform an additional stage of manual verification. A trained audio-visual annotator
262 reviews all candidate samples and applies the following criteria: (1) **Clear temporal cues in the
263 video:** The visual channel must present actions with identifiable rhythmic or temporal structure,
264 allowing annotators to infer the timing of corresponding sound events (e.g., excluding horn sounds
265 without visible motion cues). (2) **On-screen sound sources:** All target sound events must be phys-
266 ically present in the associated video frames, ensuring that the model is not required to separate
267

Table 1: Comparison of visually-queried sound separation performance on MUSIC-Clean, VGGSound-Clean, and VGGSound-Hard (VG-Hard). The evaluation considers semantic consistency between audio–audio (S_{A-A}), semantic consistency between audio–visual (S_{A-V}), and temporal consistency between audio–visual (T_{A-V}) to assess the quality of the separated results. \dagger Since Davis is originally trained on different datasets, we retrained their models on the same dataset to ensure a fair comparison.

Method	Temp.	VGGSound-Clean			Music-Clean			VS-Hard	
		Align	$S_{A-A} \uparrow$	$S_{A-V} \uparrow$	$T_{A-V} \uparrow$	$S_{A-A} \uparrow$	$S_{A-V} \uparrow$	$T_{A-V} \uparrow$	$T_{A-V} \uparrow$
Target Audio		\times	100.00	39.33	95.83	100.00	37.10	82.22	94.07
Mixed Audio		\times	63.20	19.71	61.46	52.96	15.18	28.89	73.73
CLIPSEP (Dong et al., 2022)		\times	66.74	24.21	79.17	60.59	21.42	51.11	85.59
i-Query (Chen et al., 2023)		\times	68.14	26.93	80.78	66.29	24.46	64.21	79.52
OmniSep (Cheng et al., 2024)		\times	70.83	27.57	81.25	67.67	25.74	68.89	76.27
\dagger Davis (Huang et al., 2024)		\times	62.53	23.18	74.39	61.32	22.49	56.47	74.13
\dagger Davis-flow (Huang et al., 2025)		\times	65.82	24.21	82.32	69.21	27.76	65.71	76.27
AlignSep (ours)		✓	73.38	27.89	96.88	72.28	28.92	66.67	95.76

Table 2: Mean Opinion Score (MOS) across four evaluation dimensions: Noise Residuals (NR), Audio-Visual Consistency (AVC), Audio Quality (AQ), and Overall Score (OS).

Method	VGGSound-Clean				Music-Clean				VGGSound-Hard			
	NR	AVC	AQ	OA	NR	AVC	AQ	OA	NR	AVC	AQ	OA
ClipSep	3.31	3.31	3.31	3.85	2.91	3.91	3.82	3.55	3.57	4.36	4.29	4.14
OmniSep	3.62	3.69	3.85	3.62	4.09	4.19	3.82	4.01	3.29	4.29	4.21	4.07
AlignSep	4.23	4.53	4.08	4.31	3.82	4.27	4.18	4.18	4.21	4.64	4.21	4.43

sounds originating off-screen. After this filtering process, we obtain 118 high-quality audio–visual pairs that exhibit strong semantic homogeneity yet clearly distinct temporal patterns, forming the final VGGSound-Hard benchmark.

5 EXPERIMENTS

5.1 BENCHMARKING VIDEO-QUERIED SOUND SEPARATION

Video-queried sound separation (VQSS) poses unique challenges and requires dedicated evaluation methodologies. Unlike conventional source separation, which primarily focuses on recovering semantically correct signals, VQSS additionally demands that the separated audio be temporally aligned with the visual stream. For instance, even if a separated sound is semantically consistent with the scene, it should not be preserved if it is not actually produced by the objects in the video. Existing benchmarks fail to capture this dual requirement. To address this limitation, we establish a new benchmark that introduces tailored evaluation metrics and dataset settings for VQSS.

Evaluation Metrics. Conventional source separation is usually assessed with reconstruction-based metrics such as SDR (Vincent et al., 2006), which correlate poorly with human perception (Le Roux et al., 2019; Cartwright et al., 2018). The gap is even larger for generative methods (Hai et al., 2024; Yuan et al., 2024), where minor waveform deviations can lead to large but perceptually irrelevant errors. We therefore adopt a comprehensive evaluation protocol covering two dimensions: (1) Semantic Alignment: CLAP for audio–audio (A–A) and ImageBind for audio–visual (A–V) consistency; (2) Temporal Synchronization: alignment accuracy (Acc) (Luo et al., 2023), following Video-to-Audio evaluation (Xing et al., 2024; Wang et al., 2025).

To bridge the gap between objective scores and human perception, we further conduct Mean Opinion Score (MOS) evaluations, where human raters assess four aspects of the generated outputs: Noise Residuals (NR), Audio-Visual Consistency (AVC), Audio Quality (AQ), and Overall Score (OS).

MOS provides complementary insights into perceptual quality and cross-modal coherence, ensuring a more faithful assessment of real-world performance. The detailed evaluation protocol and rating procedure are provided in the Appendix B.

Datasets. As an early effort in VQSS, Dong et al. (2022) curated VGG SOUND-Clean and MUSIC-Clean, where target and interference sounds are drawn from different categories, representing relatively simple separation cases. To better reflect real-world scenarios—where overlapping sounds often come from the same class and are harder to disentangle—we introduce VGG SOUND-Hard, a new benchmark in which both target and interference sounds are from the same category and the target audio must be highly temporally aligned with the visual stream. This provides a more realistic and challenging testbed for advancing VQSS research.

5.2 IMPLEMENTATION DETAILS

Following recent video-to-audio (V2A) works (Luo et al., 2023; Wang et al., 2025), we downsampled all audio signals into 16 kHz and converted them to Mel-spectrograms with 80 frequency bins and a hop size of 256. All videos were downsampled to 4 FPS. All data samples were truncated into 8-second clips for both training and inference. The transformer architecture in our vector field estimator comprises 4 layers with a hidden dimension of 576. For waveform synthesis, we used a pretrained BigVGAN vocoder (Lee et al., 2022). Additional implementation details are provided in Appendix A.

5.3 MAIN RESULTS

Table 1 presents the quantitative results of visual-queried sound separation on MUSIC-Clean, VGGSound-Clean, and the more challenging VGGSound-Hard benchmark. Compared with the baselines, CLIPSep (Dong et al., 2022) and OmniSep (Cheng et al., 2024), our proposed **AlignSep** achieves consistent and notable improvements across all datasets. On MUSIC-Clean and VGGSound-Clean, AlignSep yields higher scores in both semantic consistency (S_{A-A} , S_{A-V}) and temporal alignment (T_{A-V}), demonstrating its capability to leverage both semantic and temporal cues. Particularly on the VGG SOUND-Clean benchmark, AlignSep reaches 96.88% in T_{A-V} , significantly surpassing the baselines, while on VGGSound-Hard it maintains a strong 95.76% despite the increased difficulty. In contrast, while OmniSep improves semantic consistency compared with CLIPSep, its performance on VGGSound-Hard drops to 76.27% T_{A-V} , suggesting limited capacity in modeling temporal relationships under complex acoustic-visual mixtures. These results collectively demonstrate that AlignSep not only strengthens semantic alignment but also effectively captures fine-grained temporal correspondence, leading to superior sound separation quality across both clean and challenging benchmarks.

To further assess perceptual quality, Table 2 reports Mean Opinion Scores (MOS) across four human evaluation dimensions: Noise Residuals (NR), Audio-Visual Consistency (AVC), Audio Quality (AQ), and Overall Score (OA). AlignSep consistently outperforms both CLIPSep and OmniSep across all datasets and evaluation aspects. On Music-Clean, it achieves the highest ratings in every dimension (e.g., 4.53 AVC, 4.31 OA), highlighting its effectiveness in producing clean, temporally aligned, and perceptually natural audio. On VGG SOUND-Clean, while OmniSep scores highest in NR (4.09), AlignSep leads in AVC (4.27), AQ (4.18), and OA (4.18), suggesting better perceived audio-visual coherence. For the most challenging VGGSound-Hard set, AlignSep again delivers the best overall score (4.43), showing robustness even under complex and ambiguous conditions. Together, these subjective results corroborate the quantitative gains, indicating that AlignSep not only improves alignment metrics but also translates into better human-perceived separation quality.

5.4 TEMPORALLY-ALIGNED VIDEO-QUERIED SOUND SEPARATION

To compare the temporal alignment ability of different VQSS methods, we evaluate their performance when varying the number of reference video frames used as queries. For OmniSep and CLIPSep, which do not inherently model temporal dynamics, we adapt them by segmenting the mixed audio according to each frame’s semantic information, thereby enforcing temporal alignment. Figure 3 illustrates the impact of reference frame rate (FPS) on alignment accuracy across different

378
 379
 380
 381
 382
 383 Table 3: Evaluation of different denoising steps on VGGSound-Clean, MUSIC-VGGSound, and
 384 VGGSound-Hard. We report ImageBind similarity, CLAPScore, and alignment accuracy (Align-
 385 nAcc). The last two columns present inference time and corresponding throughput (FPS). Best
 386 results are highlighted in **bold**.
 387
 388
 389
 390
 391
 392

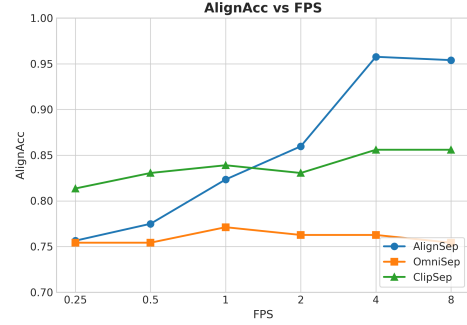
Method	VGGSound-Clean			Music-Clean			VS-Hard	FPS↑
	$S_{A-V} \uparrow$	$S_{A-A} \uparrow$	$T_{A-V} \uparrow$	$S_{A-V} \uparrow$	$S_{A-A} \uparrow$	$T_{A-V} \uparrow$	$T_{A-V} \uparrow$	
AlignSep(Step=5)	25.11	64.47	85.42	22.13	62.17	44.44	88.14	5.56
AlignSep(Step=10)	26.66	69.86	92.71	24.92	68.51	53.33	94.07	4.00
AlignSep(Step=25)	27.89	73.38	96.88	28.92	72.28	66.67	95.76	2.17
AlignSep(Step=50)	28.12	73.50	95.83	30.70	72.13	68.89	93.22	1.35
AlignSep(Step=100)	2756	73.64	96.88	30.88	72.80	68.89	93.22	0.72
OmniSep	27.57	70.83	81.25	25.74	67.67	68.89	76.27	11.2
AlignSep _{Rectified Flow} ^{step=100}	21.39	57.36	84.38	21.41	49.76	46.67	92.37	0.77

393
 394
 395 methods. AlignSep shows a clear upward trend: as the FPS increases, its performance steadily im-
 396 proves and saturates at higher frame rates, rising from about 0.76 at 0.25 FPS to nearly 0.95 at 4 FPS.
 397 These results demonstrate that AlignSep effec-
 398 tively leverages fine-grained temporal cues to
 399 enhance separation quality.

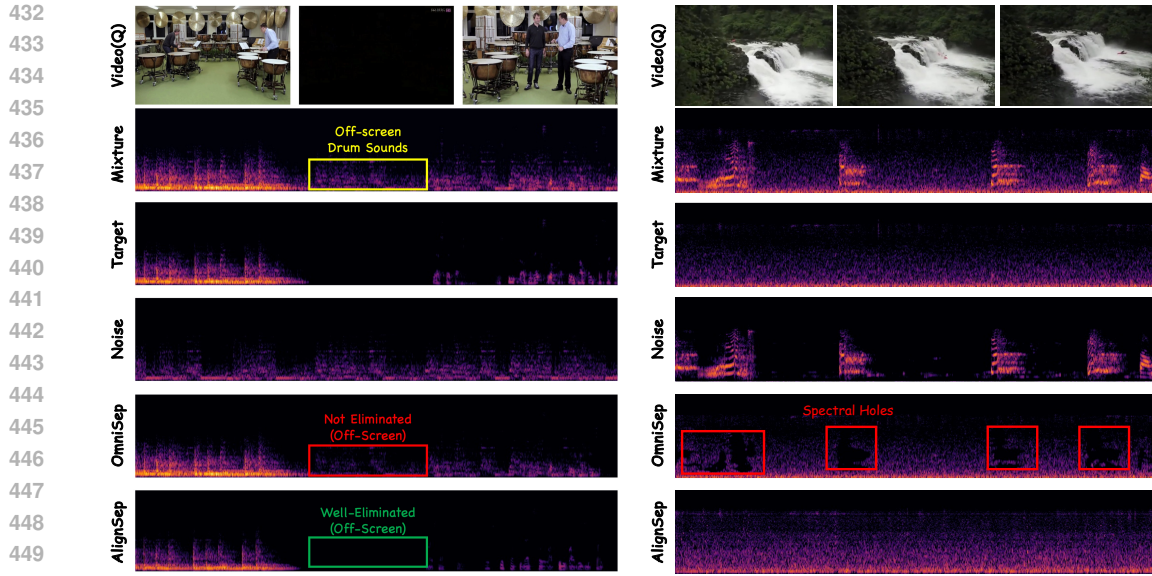
400 In contrast, ClipSep shows an almost flat curve
 401 around 0.81 across all frame rates. These
 402 image-based methods rely solely on semantic
 403 modeling and lack temporal information, re-
 404 sulting in weak dependency on visual tempo-
 405 ral resolution and a clear limitation in exploit-
 406 ing alignment signals. OmniSep, while bene-
 407 fiting from enhanced semantic alignment that
 408 improves its performance on simpler datasets
 409 such as VGGSound-Clean, struggles on more
 410 challenging benchmarks like VGGSound-Hard
 411 that demand temporal modeling. Its empha-
 412 sis on cross-modal semantic alignment further
 413 restricts the modeling of temporal correspon-
 414 dence, leading to even lower separation perfor-
 415 mance in such scenarios.

416 5.5 PERFORMANCE AND EFFICIENCY DISCUSSION IN SOUND SEPARATION

417
 418 **Generative methods meet the core requirements of VQSS.** Although generative sound separa-
 419 tion methods are slightly slower than traditional mask-based approaches, their ability to directly gen-
 420 erate waveforms makes them naturally suited for Video-Queried Sound Separation (VQSS). They
 421 effectively address two of the most critical challenges in this task: **(1) Disentangling overlapping**
 422 **signals.** The objective of VQSS is to isolate the target audio source from a mixture, guided by
 423 visual input. Generative models perform iterative inference with cross-modal conditioning at each
 424 step, allowing them to enforce mixture and phase consistency. This iterative refinement gradu-
 425 ally routes ambiguous energy to the correct source and reduces leakage. As shown in the results,
 426 AlignSep’s performance improves steadily with more denoising steps—on VGGSound-Clean, the
 427 audio–visual semantic score (S_{A-V}) increases from $64.47 \rightarrow 73.38 \rightarrow 73.64$ as the number of steps
 428 increases from $5 \rightarrow 25 \rightarrow 100$, while the temporal alignment score (T_{A-V}) reaches 96.88 at both 25
 429 and 100 steps. In contrast, traditional mask-based methods struggle to separate sources with simi-
 430 lar frequency bands and often suffer from severe separation artifacts, leading to degraded perceptual
 431 quality. **(2) Capturing fine-grained temporal alignment.** VQSS depends heavily on frame-level
 432 temporal cues, such as lip movements, object collisions, and transitions in and out of the frame.
 433 Traditional methods like OmniSep have limited capacity to model such fine temporal structure.



434
 435
 436
 437
 438 Figure 3: Comparison of sound separation perfor-
 439 mance with different levels of temporal informa-
 440 tion on VGGSound-Hard. OmniSep represents
 441 the performance when relying solely on semantic
 442 information. The x-axis indicates the number of
 443 video frames per second (FPS) used for VQSS.



(a) Temporal misalignment issue.

(b) Spectral holes issue.

Figure 4: Qualitative comparison of VQSS. (a) illustrates a temporal misalignment case, while (b) demonstrates the spectral holes artifact. We highlight the critical regions using different colors.

In comparison, conditional generative models can explicitly incorporate temporal information and refine separation results accordingly across iterations. With schedulable guidance, they can progressively enhance temporal alignment. For example, on the VS-Hard benchmark, AlignSep achieves a high alignment score of $T_{A-V} = 95.76$ with just 25 inference steps.

Traditional Rectified-flow acceleration struggles in VQSS. While *Rectified Flow* (RF) achieves fast and deterministic sampling by straightening the generative trajectory into a smooth ODE path (Lipman et al., 2022), its effectiveness diminishes in complex multi-conditioned settings such as VQSS. In VQSS, the model is required to condition jointly on an audio mixture m and a sequence of video frames $v_{1:T}$, and to perform time–frequency–object routing, i.e., assigning acoustic energy to the correct visual source over time.

This results in a posterior distribution $p(s | m, v_{1:T})$ that is highly multi-modal and piecewise non-smooth, often exhibiting discrete bifurcations and high-curvature transport paths. Under such structure, a single deterministic trajectory—as used in RF—tends to bias toward high-density regions and effectively averages across modes. Moreover, RF lacks the iterative correction mechanism found in diffusion models—specifically, the loop of denoising followed by consistency projection. This feedback loop is essential for correcting early assignment errors in multi-modal generation tasks. As a consequence, RF struggles to represent the complex conditional structure in VQSS, often leading to misalignment between generated results and the conditioning inputs. As shown in Table 3, this results in significantly lower performance: RF (with 100 sampling steps) achieves $S_{A-V} = 57.36$, markedly below the 73.64 achieved by the diffusion-based AlignSep model—despite comparable inference speeds under efficient samplers.

VQSS requires fewer sampling steps than other generation tasks. Unlike other conditional generation tasks (e.g., text-to-audio synthesis), **Visual-Query Source Separation** (VQSS) benefits from strong conditioning priors: the audio mixture already contains much of the target source, and the accompanying video provides frame-level constraints. As a result, many inference steps are unnecessary to achieve high-quality separation. In our experiments, using only 25 sampling steps yields an excellent trade-off between quality and efficiency—achieving $T_{A-V} = 96.88$ on VGG SOUND-Clean and 95.76 on VS-Hard, while running at 2.17 FPS (approximately 3× faster than the 100-step setting, which runs at 0.72 FPS). For more real-time scenarios, even 10 steps suffice to maintain strong alignment (e.g., $T_{A-V} = 92.71$ on VGG SOUND-Clean and 94.07 on VS-Hard), achieving 4.00 FPS. Beyond 25 steps, the gains in quality are marginal, while throughput degrades significantly (e.g., 1.35 FPS at 50 steps, 0.72 FPS at 100). We conclude that 25 steps strike

486 a practical balance between separation quality and inference efficiency, making it a strong candidate
 487 for deployment in real-world applications.
 488

489 **5.6 QUALITATIVE RESULTS**
 490

491 To provide a more intuitive illustration of AlignSep’s separation capability, we present qualitative
 492 comparisons with different VQSS methods in Figure 4. As shown in Figure 4a, when temporal cues
 493 between audio and video are misaligned, conventional semantics-based separation methods often
 494 fail to suppress irrelevant sounds. For example, although the drumming action in the video has al-
 495 ready stopped, OmniSep still produces drum sounds (red regions). In contrast, AlignSep effectively
 496 leverages cross-modal correspondence and avoids generating spurious signals (green regions), sep-
 497 arating audio strictly in accordance with the drumming rhythm. In Figure 4b, we highlight the
 498 spectral holes artifact, a common issue in mask-based separation methods when handling overlap-
 499 ping signals. While traditional approaches struggle to preserve continuity under such conditions
 500 (red regions), AlignSep mitigates these artifacts through its generative framework, yielding more
 501 complete and natural separation results. Additional qualitative examples are provided on our project
 502 page <https://AlignSep.github.io>.
 503

503 **6 CONCLUSION**
 504

505 In this work, we introduced AlignSep, the first generative framework for Video Query Sound Sep-
 506 aration (VQSS) based on flow matching. By integrating temporal consistency mechanisms and a gen-
 507 erative separation paradigm, AlignSep effectively addresses key challenges such as spectral holes,
 508 hallucination artifacts, and incomplete alignment. Our in-depth analysis reveals the fundamental
 509 differences between traditional single-conditioned flow matching tasks (e.g., text-to-audio) and the
 510 multi-conditioned generation setting of VQSS. To facilitate rigorous evaluation, we also constructed
 511 a challenging benchmark, VGGSound-Hard, composed of samples with homogeneous interference
 512 where temporal grounding is critical for successful separation. Extensive experiments demonstrate
 513 that AlignSep achieves state-of-the-art performance both quantitatively and perceptually across a
 514 range of benchmarks, validating its robustness and practical applicability.
 515

516 **ETHICAL CONSIDERATIONS**
 517

518 Our work focuses on the development of a generative audiovisual source separation system, which
 519 aims to improve perceptual quality and alignment between sound and vision. While this technology
 520 has potential applications in video editing, accessibility, and content understanding, we acknowledge
 521 potential misuse such as manipulation or deepfake-style content generation. To mitigate such risks,
 522 we do not train or release models for identity synthesis or cross-modal generation beyond the scope
 523 of separation. All training data used in this work (MUSIC, VGGSound, and our VGGSound-Hard
 524 subset) are publicly available datasets collected for research purposes. No personally identifiable
 525 information (PII) is included, and we ensure compliance with the licenses and usage guidelines of
 526 each dataset. Human evaluations (e.g., MOS) were conducted anonymously with informed consent.
 527 We encourage responsible usage of this technology and explicitly discourage applications involving
 528 surveillance, impersonation, or deceptive audio generation.
 529

530 **REPRODUCIBILITY STATEMENT**
 531

532 All code, pretrained models, and related resources will be publicly released upon paper acceptance
 533 under a permissive license, to encourage further research and community adoption. Detailed im-
 534 plementation settings and training protocols are thoroughly documented in the paper to facilitate
 535 reproducibility and independent verification.
 536

537 **REFERENCES**
 538

539 Mark Cartwright, Bryan Pardo, and Gautham J Mysore. Crowdsourced pairwise-comparison for
 540 source separation evaluation. In *2018 ieee international conference on acoustics, speech and*
541 signal processing (icassp), pp. 606–610. IEEE, 2018.

540 Honglie Chen, Weidi Xie, Andrea Vedaldi, and Andrew Zisserman. Vggsound: A large-scale audio-
 541 visual dataset. In *ICASSP 2020-2020 IEEE International Conference on Acoustics, Speech and*
 542 *Signal Processing (ICASSP)*, pp. 721–725. IEEE, 2020.

543

544 Jiaben Chen, Renrui Zhang, Dongze Lian, Jiaqi Yang, Ziyao Zeng, and Jianbo Shi. iquery: Instru-
 545 ments as queries for audio-visual sound separation. In *Proceedings of the IEEE/CVF Conference*
 546 *on Computer Vision and Pattern Recognition*, pp. 14675–14686, 2023.

547

548 Ke Chen, Jiaqi Su, and Zeyu Jin. Mdx-gan: Enhancing perceptual quality in multi-class source
 549 separation via adversarial training. In *ICASSP 2024-2024 IEEE International Conference on*
 550 *Acoustics, Speech and Signal Processing (ICASSP)*, pp. 741–745. IEEE, 2024.

551

552 Xize Cheng, Siqi Zheng, Zehan Wang, Minghui Fang, Ziang Zhang, Rongjie Huang, Ziyang Ma,
 553 Shengpeng Ji, Jialong Zuo, Tao Jin, et al. Omnisep: Unified omni-modality sound separation with
 554 query-mixup. *arXiv preprint arXiv:2410.21269*, 2024.

555

556 Alexandre Défossez, Nicolas Usunier, Léon Bottou, and Francis Bach. Demucs: Deep extractor for
 557 music sources with extra unlabeled data remixed. *arXiv preprint arXiv:1909.01174*, 2019.

558

559 Hao-Wen Dong, Naoya Takahashi, Yuki Mitsuji, Julian McAuley, and Taylor Berg-Kirkpatrick.
 560 Clipsep: Learning text-queried sound separation with noisy unlabeled videos. *arXiv preprint*
 561 *arXiv:2212.07065*, 2022.

562

563 Ruohan Gao and Kristen Grauman. Visualvoice: Audio-visual speech separation with cross-
 564 modal consistency. In *2021 IEEE/CVF Conference on Computer Vision and Pattern Recognition*
 565 (*CVPR*), pp. 15490–15500. IEEE, 2021.

566

567 Jort F Gemmeke, Daniel PW Ellis, Dylan Freedman, Aren Jansen, Wade Lawrence, R Channing
 568 Moore, Manoj Plakal, and Marvin Ritter. Audio set: An ontology and human-labeled dataset for
 569 audio events. In *2017 IEEE international conference on acoustics, speech and signal processing*
 570 (*ICASSP*), pp. 776–780. IEEE, 2017.

571

572 Jiarui Hai, Helin Wang, Dongchao Yang, Karan Thakkar, Najim Dehak, and Mounya Elhilali. Dpm-
 573 tse: A diffusion probabilistic model for target sound extraction. In *ICASSP 2024-2024 IEEE*
 574 *International Conference on Acoustics, Speech and Signal Processing (ICASSP)*, pp. 1196–1200.
 575 IEEE, 2024.

576

577 Jiaming Han, Renrui Zhang, Wenqi Shao, Peng Gao, Peng Xu, Han Xiao, Kaipeng Zhang, Chris Liu,
 578 Song Wen, Ziyu Guo, et al. Imagebind-llm: Multi-modality instruction tuning. *arXiv preprint*
 579 *arXiv:2309.03905*, 2023.

580

581 John R Hershey, Zhuo Chen, Jonathan Le Roux, and Shinji Watanabe. Deep clustering: Discrim-
 582 inative embeddings for segmentation and separation. In *2016 IEEE international conference on*
 583 *acoustics, speech and signal processing (ICASSP)*, pp. 31–35. IEEE, 2016.

584

585 Wei-Ning Hsu, Tal Remez, Bowen Shi, Jacob Donley, and Yossi Adi. Revise: Self-supervised
 586 speech resynthesis with visual input for universal and generalized speech regeneration. In *Pro-
 587 ceedings of the IEEE/CVF Conference on Computer Vision and Pattern Recognition*, pp. 18795–
 588 18805, 2023.

589

590 Chao Huang, Susan Liang, Yapeng Tian, Anurag Kumar, and Chenliang Xu. High-quality visually-
 591 guided sound separation from diverse categories. In *Proceedings of the Asian Conference on*
 592 *Computer Vision*, pp. 35–49, 2024.

593

594 Chao Huang, Susan Liang, Yapeng Tian, Anurag Kumar, and Chenliang Xu. High-quality sound
 595 separation across diverse categories via visually-guided generative modeling. *arXiv preprint*
 596 *arXiv:2509.22063*, 2025.

597

598 Rongjie Huang, Jiawei Huang, Dongchao Yang, Yi Ren, Luping Liu, Mingze Li, Zhenhui Ye, Jinglin
 599 Liu, Xiang Yin, and Zhou Zhao. Make-an-audio: Text-to-audio generation with prompt-enhanced
 600 diffusion models. In *International Conference on Machine Learning*, pp. 13916–13932. PMLR,
 601 2023.

594 Ilya Kavalerov, Scott Wisdom, Hakan Erdogan, Brian Patton, Kevin Wilson, Jonathan Le Roux, and
 595 John R Hershey. Universal sound separation. In *2019 IEEE Workshop on Applications of Signal*
 596 *Processing to Audio and Acoustics (WASPAA)*, pp. 175–179. IEEE, 2019.

597

598 Qiuqiang Kong, Yuxuan Wang, Xuchen Song, Yin Cao, Wenwu Wang, and Mark D Plumbley.
 599 Source separation with weakly labelled data: An approach to computational auditory scene anal-
 600 ysis. In *ICASSP 2020-2020 IEEE International Conference on Acoustics, Speech and Signal*
 601 *Processing (ICASSP)*, pp. 101–105. IEEE, 2020.

602 Trausti T Kristjansson, John R Hershey, Peder A Olsen, Steven J Rennie, and Ramesh A Gopinath.
 603 Super-human multi-talker speech recognition: the ibm 2006 speech separation challenge system.
 604 In *Interspeech*, volume 12, pp. 155. Citeseer, 2006.

605

606 Jonathan Le Roux, Scott Wisdom, Hakan Erdogan, and John R Hershey. Sdr-half-baked or well
 607 done? In *ICASSP 2019-2019 IEEE International Conference on Acoustics, Speech and Signal*
 608 *Processing (ICASSP)*, pp. 626–630. IEEE, 2019.

609 Sang-gil Lee, Wei Ping, Boris Ginsburg, Bryan Catanzaro, and Sungroh Yoon. Bigvgan: A universal
 610 neural vocoder with large-scale training. *arXiv preprint arXiv:2206.04658*, 2022.

611

612 Songju Lei, Xize Cheng, Mengjiao Lyu, Jianqiao Hu, Jintao Tan, Runlin Liu, Lingyu Xiong, Tao Jin,
 613 Xiandong Li, and Zhou Zhao. Uni-dubbing: Zero-shot speech synthesis from visual articulation.
 614 In Lun-Wei Ku, Andre Martins, and Vivek Srikanth (eds.), *Proceedings of the 62nd Annual Meet-
 615 ing of the Association for Computational Linguistics (Volume 1: Long Papers)*, pp. 10082–10099,
 616 Bangkok, Thailand, August 2024. Association for Computational Linguistics. doi: 10.18653/v1/
 617 2024.acl-long.543. URL <https://aclanthology.org/2024.acl-long.543/>.

618 Kai Li, Runxuan Yang, and Xiaolin Hu. An efficient encoder-decoder architecture with top-down
 619 attention for speech separation. *arXiv preprint arXiv:2209.15200*, 2022.

620 Xiang Li, Yiwen Wang, Yifan Sun, Xihong Wu, and Jing Chen. Pgss: pitch-guided speech sepa-
 621 ration. In *Proceedings of the AAAI Conference on Artificial Intelligence*, volume 37, pp. 13130–
 622 13138, 2023.

623 Yaron Lipman, Ricky TQ Chen, Heli Ben-Hamu, Maximilian Nickel, and Matt Le. Flow matching
 624 for generative modeling. *arXiv preprint arXiv:2210.02747*, 2022.

625

626 Haohe Liu, Zehua Chen, Yi Yuan, Xinhao Mei, Xubo Liu, Danilo Mandic, Wenwu Wang, and
 627 Mark D Plumbley. Audioldm: Text-to-audio generation with latent diffusion models. *arXiv*
 628 *preprint arXiv:2301.12503*, 2023a.

629

630 Xubo Liu, Haohe Liu, Qiuqiang Kong, Xinhao Mei, Jinzheng Zhao, Qiushi Huang, Mark D Plumb-
 631 ley, and Wenwu Wang. Separate what you describe: Language-queried audio source separation.
 632 *arXiv preprint arXiv:2203.15147*, 2022.

633 Xubo Liu, Qiuqiang Kong, Yan Zhao, Haohe Liu, Yi Yuan, Yuzhuo Liu, Rui Xia, Yuxuan
 634 Wang, Mark D Plumbley, and Wenwu Wang. Separate anything you describe. *arXiv preprint*
 635 *arXiv:2308.05037*, 2023b.

636

637 Xubo Liu, Qiuqiang Kong, Yan Zhao, Haohe Liu, Yi Yuan, Yuzhuo Liu, Rui Xia, Yuxuan Wang,
 638 Mark D Plumbley, and Wenwu Wang. Separate anything you describe. *IEEE/ACM Transactions*
 639 *on Audio, Speech, and Language Processing*, 2024.

640 Simian Luo, Chuanhao Yan, Chenxu Hu, and Hang Zhao. Diff-foley: Synchronized video-to-audio
 641 synthesis with latent diffusion models. *Advances in Neural Information Processing Systems*, 36:
 642 48855–48876, 2023.

643

644 Yi Luo and Jianwei Yu. Music source separation with band-split rnn. *IEEE/ACM Transactions on*
 645 *Audio, Speech, and Language Processing*, 2023.

646 Hao Ma, Zhiyuan Peng, Mingjie Shao, Ju Liu, Xu Li, and Xixin Wu. Clapsep: Leveraging con-
 647 trastive pre-trained models for multi-modal query-conditioned target sound extraction. *arXiv*
 648 *preprint arXiv:2402.17455*, 2024.

648 Ethan Manilow, Patrick O'Reilly, Prem Seetharaman, and Bryan Pardo. Source separation by steering
 649 pretrained music models. In *ICASSP 2022-2022 IEEE International Conference on Acoustics,
 650 Speech and Signal Processing (ICASSP)*, pp. 126–130. IEEE, 2022.

651

652 Tsubasa Ochiai, Marc Delcroix, Yuma Koizumi, Hiroaki Ito, Keisuke Kinoshita, and Shoko Araki.
 653 Listen to what you want: Neural network-based universal sound selector. *arXiv preprint
 654 arXiv:2006.05712*, 2020.

655

656 Samuel Pegg, Kai Li, and Xiaolin Hu. Rtfs-net: Recurrent time-frequency modelling for efficient
 657 audio-visual speech separation. *arXiv preprint arXiv:2309.17189*, 2023.

658

659 Jordi Pons, Xiaoyu Liu, Santiago Pascual, and Joan Serrà. Gass: Generalizing audio source sepa-
 660 ration with large-scale data. In *ICASSP 2024-2024 IEEE International Conference on Acoustics,
 661 Speech and Signal Processing (ICASSP)*, pp. 546–550. IEEE, 2024.

662

663 Simon Rouard, Francisco Massa, and Alexandre Défossez. Hybrid transformers for music source
 664 separation. In *ICASSP 2023-2023 IEEE International Conference on Acoustics, Speech and Sig-
 665 nal Processing (ICASSP)*, pp. 1–5. IEEE, 2023.

666

667 Sam Roweis. One microphone source separation. *Advances in neural information processing sys-
 668 tems*, 13, 2000.

669

670 Efthymios Tzinis, Scott Wisdom, Aren Jansen, Shawn Hershey, Tal Remez, Daniel PW Ellis, and
 671 John R Hershey. Into the wild with audioscope: Unsupervised audio-visual separation of on-
 672 screen sounds. *arXiv preprint arXiv:2011.01143*, 2020.

673

674 Efthymios Tzinis, Scott Wisdom, Tal Remez, and John R Hershey. Audioscopev2: Audio-visual
 675 attention architectures for calibrated open-domain on-screen sound separation. In *European Con-
 676 ference on Computer Vision*, pp. 368–385. Springer, 2022.

677

678 Emmanuel Vincent, Rémi Gribonval, and Cédric Févotte. Performance measurement in blind audio
 679 source separation. *IEEE transactions on audio, speech, and language processing*, 14(4):1462–
 680 1469, 2006.

681

682 DeLiang Wang and Jitong Chen. Supervised speech separation based on deep learning: An overview.
 683 *IEEE/ACM Transactions on Audio, Speech, and Language Processing*, pp. 1702–1726, Oct 2018.
 684 doi: 10.1109/taslp.2018.2842159. URL [http://dx.doi.org/10.1109/taslp.2018.
 2842159](http://dx.doi.org/10.1109/taslp.2018.2842159).

685

686 Helin Wang, Dongchao Yang, Chao Weng, Jianwei Yu, and Yuexian Zou. Improving target sound
 687 extraction with timestamp information. *arXiv preprint arXiv:2204.00821*, 2022.

688

689 Helin Wang, Jiarui Hai, Yen-Ju Lu, Karan Thakkar, Mounya Elhilali, and Najim Dehak. Soloau-
 690 dio: Target sound extraction with language-oriented audio diffusion transformer. *arXiv preprint
 691 arXiv:2409.08425*, 2024a.

692

693 Xihua Wang, Yuyue Wang, Yihan Wu, Ruihua Song, Xu Tan, Zehua Chen, Hongteng Xu, and
 694 Guodong Sui. Tiva: Time-aligned video-to-audio generation. In *Proceedings of the 32nd ACM
 695 International Conference on Multimedia*, pp. 573–582, 2024b.

696

697 Yongqi Wang, Wenxiang Guo, Rongjie Huang, Jiawei Huang, Zehan Wang, Fuming You, Ruiqi
 698 Li, and Zhou Zhao. Frieren: Efficient video-to-audio generation network with rectified flow
 699 matching. *Advances in Neural Information Processing Systems*, 37:128118–128138, 2025.

700

701 Zhong-Qiu Wang, Samuele Cornell, Shukjae Choi, Younglo Lee, Byeong-Yeol Kim, and Shinji
 702 Watanabe. Tf-gridnet: Making time-frequency domain models great again for monaural speaker
 703 separation. In *ICASSP 2023-2023 IEEE International Conference on Acoustics, Speech and Sig-
 704 nal Processing (ICASSP)*, pp. 1–5. IEEE, 2023.

705

706 Scott Wisdom, Efthymios Tzinis, Hakan Erdogan, Ron Weiss, Kevin Wilson, and John Hershey.
 707 Unsupervised sound separation using mixture invariant training. *Advances in Neural Information
 708 Processing Systems*, 33:3846–3857, 2020.

702 Yazhou Xing, Yingqing He, Zeyue Tian, Xintao Wang, and Qifeng Chen. Seeing and hearing: Open-
 703 domain visual-audio generation with diffusion latent aligners. In *Proceedings of the IEEE/CVF*
 704 *Conference on Computer Vision and Pattern Recognition*, pp. 7151–7161, 2024.

706 Dong Yu, Morten Kolbæk, Zheng-Hua Tan, and Jesper Jensen. Permutation invariant training of
 707 deep models for speaker-independent multi-talker speech separation. In *2017 IEEE International*
 708 *Conference on Acoustics, Speech and Signal Processing (ICASSP)*, pp. 241–245. IEEE, 2017.

710 Yi Yuan, Xubo Liu, Haohe Liu, Mark D Plumbley, and Wenwu Wang. Flowsep: Language-queried
 711 sound separation with rectified flow matching. *arXiv preprint arXiv:2409.07614*, 2024.

713 Chenshuang Zhang, Chaoning Zhang, Mengchun Zhang, and In So Kweon. Text-to-image diffusion
 714 models in generative ai: A survey. *arXiv preprint arXiv:2303.07909*, 2023.

A IMPLEMENTATION DETAILS

720 Table 4: Architecture details of 1D VAE for spectrogram compression.
 721

722 Hyperparameter	723 1D VAE
724 Input tensor shape for 8-sec audio	(80,512)
725 Embedding dimension	20
726 Channels	224
727 Channel multiplier	1, 2, 4
728 Downsample layer position	after block 1
729 Attention layer position	after block 3
730 Output tensor shape for 8-sec audio	(20,256)

731 The detailed hyperparameters for the VAE are provided in Table 4. This one-dimensional convolutional
 732 VAE model (1D VAE) is designed to process 8-second audio clips. For an input tensor with
 733 a shape of (80, 512), the model encodes it into a compact latent representation with an embedding
 734 dimension of 20, resulting in an output tensor with a shape of (20, 256). Regarding the network
 735 architecture, the initial number of channels is set to 224, and channel multipliers of 1, 2, and 4 are
 736 used to increase the channel depth in subsequent layers. To efficiently learn a hierarchy of features,
 737 the model applies a downsampling operation after the first convolutional block and integrates an
 738 attention mechanism after the third block to better capture important acoustic features.

739 Table 5: Hyperparameters of the vector field estimator of AlignSep.
 740

741 Hyperparameter	742 AlignSep
743 Layers	4
744 Hidden dimension	576
745 Attention heads	8
746 Conv1D-FFN dimension	2,304
747 Number of parameters	158.94M

748 The vector field estimator of AlignSep is given in Table 5. It is designed as a four-layer archi-
 749 tecture with a hidden dimension of 576, eight attention heads, and a Conv1D-based feed-forward
 750 network (FFN) with an intermediate dimension of 2,304, totaling approximately 158.94M parame-
 751 ters. Notably, the hidden size is chosen to align with the feature representations: the generated audio
 752 is represented with 288 dimensions, while both the video and the reference audio are represented
 753 with 144 dimensions. This configuration ensures that the model effectively captures and enriches
 754 the details of the generated audio by integrating complementary cues from the visual and reference
 755 audio modalities. Moreover, we concatenate all information together to achieve better temporal
 consistency.

756 B MOS EVALUATION

758 We conducted a Mean Opinion Score (MOS) evaluation to assess the perceptual quality of the generated
 759 audio across four dimensions: Noise Residuals, Audio-Visual Consistency, Audio Quality,
 760 and Overall Score. We display the rating criteria of MOS in Table 7.

- 762 • Participants: 3 proficient annotator were recruited, with diverse backgrounds to reduce bias.
 763 Each participant was compensated for their time.
- 764 • Samples: For each method and each subset, we randomly selected 100 audio clips. Each
 765 participant was presented with the same randomized set of samples to ensure consistency.
- 766 • Scoring Protocol: Listeners rated each sample on a 5-point Likert scale (1 = Very Poor, 5 =
 767 Excellent) according to the four predefined dimensions (see Table 2). Detailed definitions
 768 of each dimension were provided beforehand to calibrate annotators' understanding.
- 769 • Randomization: The order of both methods and samples was randomized per participant to
 770 avoid ordering effects or bias toward specific systems.
- 771 • Aggregation: For each dimension, we report the mean and standard deviation across all
 772 raters and samples. Scores are averaged first across raters for each sample, and then across
 773 samples to obtain the final MOS.

775 Table 6: Mean Opinion Score (MOS) Rating Criteria

777 Dimension	778 Score	779 Description
780 Noise Residuals	1	Very Noisy: Strong background noise that significantly affects intelligibility.
	2	Noisy: Noticeable noise, but speech or content remains intelligible.
	3	Acceptable: Minor noise present, generally tolerable.
	4	Clean: Little to no residual noise; very mild artifacts may exist.
	5	Very Clean: Completely free of noise or artifacts.
785 Audio-Visual Consistency	1	Inconsistent: Completely misaligned with visual content or scene context.
	2	Low Consistency: Partially related, but mostly inconsistent.
	3	Moderate: Generally acceptable but with clear mismatches.
	4	Consistent: Mostly aligned with minor inconsistencies.
	5	Perfectly Consistent: Fully synchronized and semantically coherent with visual content.
791 Audio Quality	1	Very Poor: Severely distorted, broken, or unnatural audio.
	2	Poor: Audible artifacts and degraded quality.
	3	Fair: Intelligible but lacks clarity or sounds slightly artificial.
	4	Good: Clear and natural with minor imperfections.
	5	Excellent: Highly natural, smooth, and human-like audio quality.
795 Overall Score	1	Very Poor: Unacceptable overall experience.
	2	Poor: Noticeable flaws that degrade the overall experience.
	3	Fair: Usable but with evident limitations.
	4	Good: Overall pleasant and functional.
	5	Excellent: High-quality and highly realistic audio experience.

799 C USE OF LLM.

802 We used a large language model (LLM) solely for polishing the language of this paper.

804 D MORE EXPERIMENTS

806 D.1 ABLATION STUDY ON GENERATIVE MODEL CHOICE.

808 As shown in table 7, on VGGSound-Clean, which demands higher semantic understanding, re-
 809 placing Flow-Matching with diffusion leads to a modest performance drop, indicating that Flow-
 Matching helps improve the model's upper bound. On VGGSound-Hard, the performance drop of

810
811
812 Table 7: Ablation study on generative model choice.
813
814
815
816

Method	VS-Clean (S_{A-A})	VS-Clean (S_{A-V})	VS-Clean (T_{A-V})	VS-Hard (T_{A-V})
AlignSep	73.38	27.89	96.88	95.76
AlignSep (w/o Flow-Matching)	64.12	24.66	93.37	92.28
AlignSep (w/o CAVP)	69.21	26.76	94.71	76.27

817
818 Table 8: Ablation on different temporal fusion strategies.
819
820

Method	VS-Clean (S_{A-A})	VS-Clean (S_{A-V})	VS-Clean (T_{A-V})	VS-Hard (T_{A-V})
cross-attention	70.13	27.12	93.29	73.38
concat	73.38	27.89	96.88	95.76

821 AlignSep without Flow-Matching is minor (3.48), whereas removing CAVP causes a significant drop
822 (19.49). This demonstrates that the temporal consistency in AlignSep relies primarily on effective
823 visual temporal understanding rather than just the generative modeling method.

824
825 D.2 ABLATION ON DIFFERENT TEMPORAL FUSION STRATEGIES.

826 Temporal fusion strategy is a key factor in our task. To evaluate its impact, we compared cross-
827 attention with our concat fusion method in table 8. Results show that the two perform similarly on
828 VS-clean (semantic-oriented), but on VS-hard—where strict temporal alignment is required—cross-
829 attention fails almost entirely to capture temporal correspondence. This highlights the advantage of
830 our concat-based fusion for temporal modeling.